Available online at www.sciencedirect.com
SCIENCE DIRECT
Microelectronic Engineering 83 (2006) 1567–1570
MICROELECTRONIC ENGINEERING
www.elsevier.com/locate/mee

Self-aligned tantalum oxide nanodot arrays through anodic alumina template

Chia-Tien Wu, Fu-Hsiang Ko *, Hsin-Yen Hwang

Institute of Nanotechnology, National Chiao Tung University, Hsinchu 300, Taiwan

Available online 14 February 2006

Abstract

A novel strategy for fabricating the ordered nanodot arrays of tantalum oxide with anodic alumina film is proposed to serve the template. Anodic oxidation of Al on TaN film has been performed in oxalic acid and sulfuric acid electrolytes at various applied voltages for porous alumina formation. Anodising reaction proceeds in the sequence of growth of porous anodic alumina when the aluminum layer is consumed up to the underlying TaN, and the growth of tantalum oxide under the bottoms of the alumina pores occurred simultaneously. The nanostructure of the nanodot arrays was studied by scanning electron microscopy, and the chemical composition of nanodots was analyzed by X-ray photoelectron spectroscopy. The nanodots are composed of nonstoichiometric TaO_x. The nanodot diameter demonstrated here ranges between 15 nm and 70 nm and density ranges between $10^{11}/cm^2$ and $10^{10}/cm^2$.

Keywords: Porous alumina; Nanodot

1. Introduction

The fabrication of nanodot arrays has attracted growing interest due to their realization in functional structures and in the field of nano-devices such as optoelectronics, information storage, and sensing [1–3]. Variety of alternative methods have been proposed for the formation of nanodot arrays such as electron beam lithographic techniques, nanoimprint [4], self-assembly of nanodot from solution [5], controlled nanoparticle growth by diffusion [6], strain-induced growth [7]. However, most of these works can be applied to only limit material systems. Since the discovery of self-ordered porous alumina in 1995 by Masuda and Fukuda [8], which consists of vertical pore channel arrays with a high density hexagonal packing structure, was obtained by anodic oxidation of aluminum in an acidic electrolyte. The pore diameters are tunable in the range of ten to several hundred nanometers, and very simple formation process making porous anodic alumina an ideal template for fabricating ordered arrays of nanostructures materials such as nanowires [9,10], nanotubes [11,12], or nanodots [13,14].

In previous work, nanodots have been fabricated by anodic alumina template as mask for evaporation of nanodots onto surface [15]. This approach has been limited to deposition of nanodots by evaporation just because of poor contact between template and underlying substrate. Moreover, during anodization an alumina barrier layer is formed at the bottom of the pores which prevent nanodots deposited directly from underlying layer. In order to use the template to deposit nanodots onto the surface, the barrier layer must be removed.

In this report, we propose a novel strategy for fabricating the tantalum oxide nanodot with anodic alumina film to serve the template. Anodizing reaction proceeds in the sequence of growth of porous anodic alumina when the aluminum layer is consumed up to the underlying metal, growth of tantalum oxide under the bottom of the alumina pores occurred. Using this approach, we can achieve highly ordered arrays of tantalum oxide nanodot with a narrow size distribution and the controllable size.

* Corresponding author.
E-mail address: fhko@mail.nctu.edu.tw (F.-H. Ko).

0167-9317/$ - see front matter © 2006 Elsevier B.V. All rights reserved.
doi:10.1016/j.mee.2006.01.092

2. Experimental

A thin TaN film about 150 nm was deposited by a sputter onto cleaned 6'' Silicon wafer. Subsequently, an aluminum layer, thickness of 3 μm, was sputter-deposited onto the TaN layer. The sample was annealing at 500 °C in a vacuum furnace with H_2/N_2 purge for 4 h The wafer was then cut into piece of $3 \times 3\ cm^2$ and electropolished in a mixed solution of 10 vol% H_3PO_4 and 10 vol% H_2SO_4. A PTFE protecting ring, fixed tightly on the aluminum surface, confined the anodizing area within a circle of 1.5 cm diameter. A flake of graphite was selected for catholic electrode. Fig. 1 is the schematic diagram of fabrication of the tantalum oxide nanodot arrays. Anodization was carried out in 1.8 M sulfuric acid (under 5, 10, 15, 20, 25 and 30 V) and 0.3 M oxalic acid (under 10, 20, 30, 40, 50 and 60 V). During all anodizing process, the temperature of the electrolytes was at 3 °C and stirred adequately. The alumina film was removed in 50 vol% H_3PO_4 overnight.

Cross-section and surface morphologies of samples were observed with JEOL JSM-6500 TFE-SEM. A thin platinum layer was evaporated before SEM observation. To examine elemental composition and, the samples were analyzed by Physical Electronics ESCA PHI1600 for surface analysis. Each sample was cleaned with 5KV ion gun for 60 s.

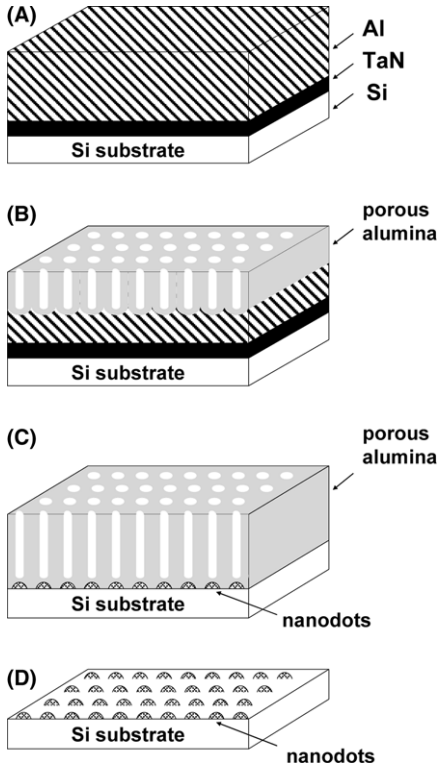

Fig. 1. Schematic diagram of fabrication of the tantalum oxide nanodot arrays: (A) prestructured Al film, (B) first anodic oxidation step, (C) second anodization step and tantalum oxide nanodot formation, and (D) tantalum oxide nanodot arrays after removing alumina films.

3. Results and discussion

Fig. 2 shows the top-view SEM image of the porous anodic alumina film anodizing in 0.3 M oxalic acid at 40 V after pore widening. The self-organized nanopores with a uniform size distribution have the interpore distance about 100 nm. Because the aluminum films in our studies were only 3 μm thick, the pore at substrate showed neither long-range order nor hexagonal arrays. It may be possible to obtain more ordered pores with a narrower size distribution by starting with thicker and fine quality films [16]. The anodic current density was steady at 8 mA/cm^2 except for initial nucleate state. When the porous alumina films had been nearly completely anodized, there was a distinct color change resulting from the transparency of the porous alumina. To ensure the process was completely anodized, the power was cut off at 0.2 mA/cm^2.

The top-view SEM images of the tantalum oxide nanodot arrays formed in various applied voltage and two different electrolytes after removing the overlying alumina film are shown in Fig. 3. Two electrolytes have been selected because of the difference in the forming voltages and electrolyte-derived species, which affected the properties of the nanodots. The population density and average diameter of nanodot were calculated and plotted in Fig. 4. The nanodot diameter ranges between 15 nm and 70 nm and density ranges between $10^{11}/cm^2$ and $10^{10}/cm^2$. The performance of the reduction in dimension and high density is superior to other reports [13–15]. The diameter and density of the nanodot can be controlled by various applied voltages. Regardless of the electrolyte, the distance between nanodots tends to be proportional to the anodizing voltages with constant of 2.5 nm/V, and this relation is in common with upper interpore distance [17]. It seems that smaller nanodot can be fabricated by lower applied voltage, but we suppose that there is a limitation

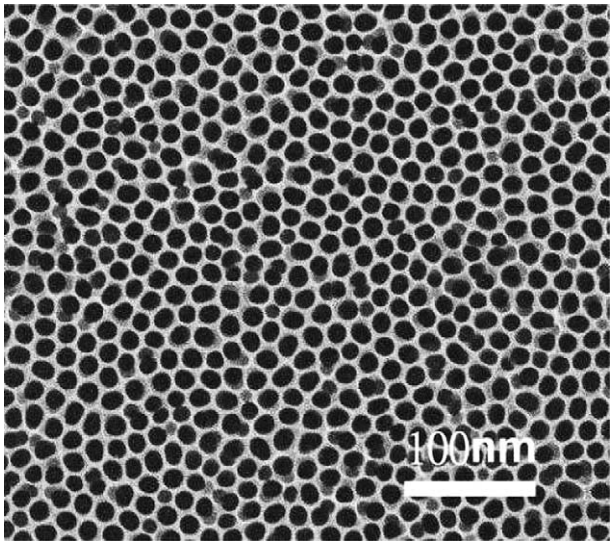

Fig. 2. Top-view SEM image of the porous anodic alumina film anodizing after pore widening in 5-wt% H_3PO_4.

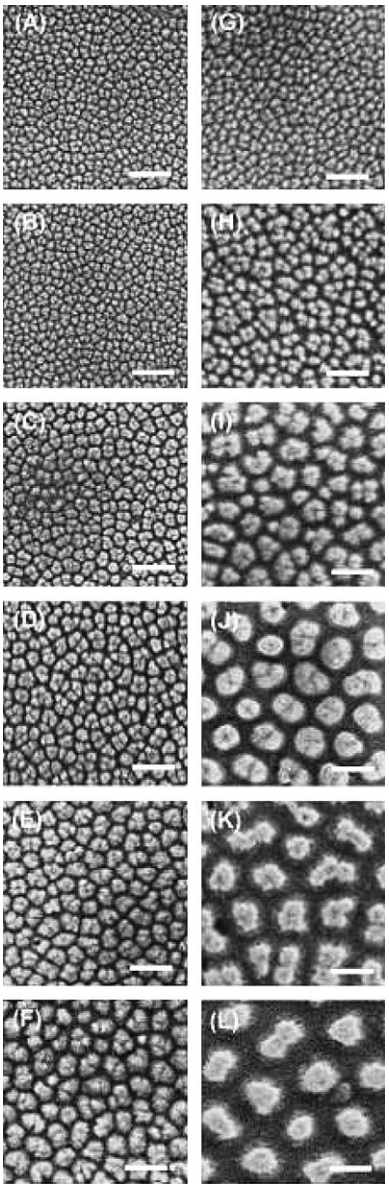

Fig. 3. SEM image of nanodot in 1.8 M sulfuric acid at (A) 5 V, (B) 10 V, (C) 15 V, (D) 20 V, (E) 25 V, (F)30 V; 0.3 M oxalic acid at (G) 10 V, (H) 20 V, (I) 30 V, (J) 40 V, (K) 50 V, (L) 60 V. The scale bar is 100 nm.

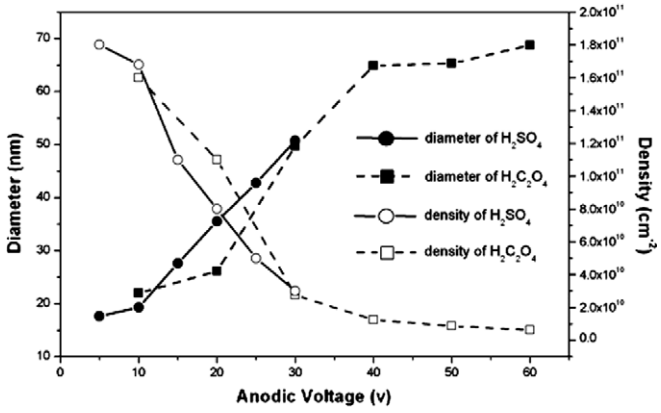

Fig. 4. The effect of applied voltage on diameter and density of tantalum oxide nanodots.

of the minimum of anodic nanodot on account of the tendency in Fig. 4 and insufficient electric field of anodization. The average diameter of self-organized nanodot arrays of tantalum oxide is relatively larger than the corresponding pore size of the alumina film without pore widening. It may be due to the radial anodizing field distribution at the TaN layer. The densities of tantalum oxide nanodot were in good agreement with the pore density of the pores of anodic alumina. Fig. 5(A) shows the SEM image of a cross-section of the nanodot in oxalic acid at 40 V, and it proved that the nanodot was formed under the bases of corresponding alumina pores while after removing the porous alumina film in Fig. 5(B).

The thickness of oxide formed per unit applied voltage of the anodizing tantalum is 1.6 (nm/V), and the ratio of oxide produced/metal consumed of Ta is 2.33 [18]. In this context, we supposed the 5-nm-thick TaN layer in $H_2C_2O_4$ electrolyte at 40 V is fully oxidized without any remaining TaN. Thus, tantalum oxide nanodot arrays were produced (Fig. 6).

It appeared Ta_2O_5 at the surface of nanodot in anodization [19]. The bombardment by ion-gun exhibited the chemical composition inside the nanodot. The obvious chemical shifts of measured spectrum of the Ta 4f doublet peaks ($4f_{7/2}$ and $4f_{5/2}$) were observed in Fig. 7. The Ta 4f peaks toward lower valence were indicated that the different oxidation states of Ta existed inside the nanodot. Surganov et al. [20] indicated that the presence of lower

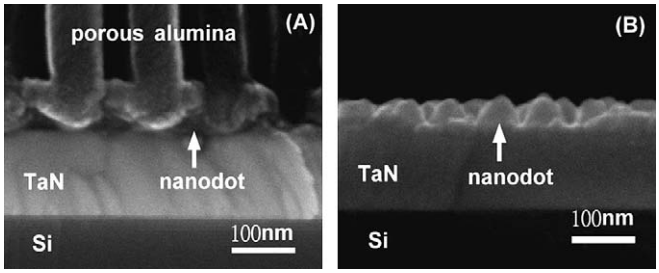

Fig. 5. (A) SEM image of a cross-section of the nanodots with overlying porous alumina film, (B) after removing alumina film.

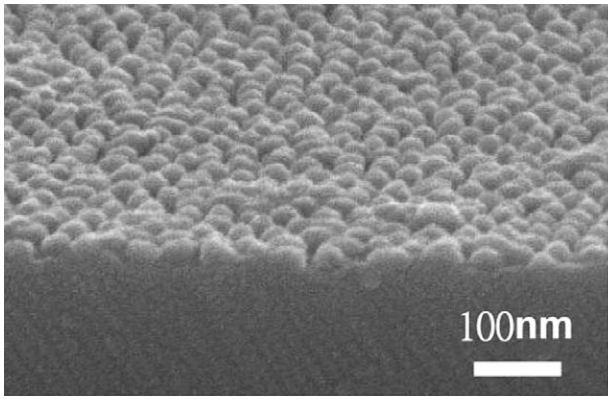

Fig. 6. SEM image of tantalum oxide nanodots arrays on the surface of the Si layer without remaining TaN.

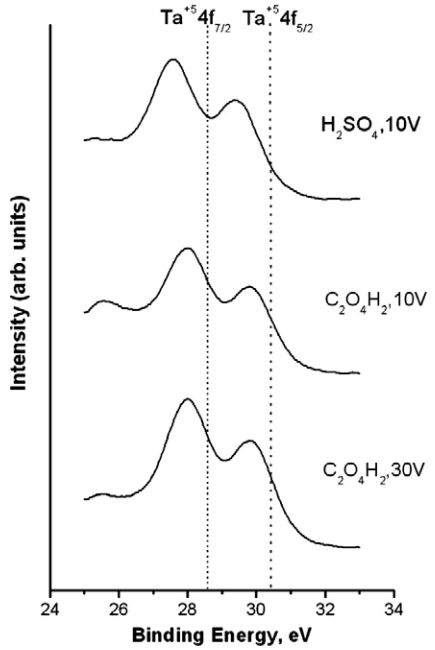

Fig. 7. XPS $4f_{7/2}$ and $4f_{5/2}$ peaks of the nanodots.

valence tantalum oxides such as TaO, TaO_2 and Ta_2O_3 in the composition of oxide columns formed in similar work. This implies the transition from stoichiometric Ta_2O_5 at the surface to tantalum nitride with the coexistence of different oxidation states of Ta.

The anodization behavior of the TaN/Al film on the silicon wafer is different from the case of the Al foil. In the first instance, the above aluminum layer oxidized to alumina, accompanied by the outward migration of Al^{3+} and inward diffusion of O^{2-} driven by the applied electric field, leading to the vertical pore channel growth. The dissolution of alumina at the alumina/electrolyte interface is in equilibrium with the growth of alumina at the Al/Al_2O_3 interface. As the oxide barrier layer at the pore bottom approaches the TaN/Al interface, the O^{2-} migrating inwards through the alumina barrier layer are continuously injected into the Ta layer and form the tantalum oxide. The underlying tantalum oxide by O^{2-} transported through/from the barrier layer of the initially formed porous alumina without direct contact of tantalum with the electrolyte. The anodic reaction of TaN results in the formation of tantalum oxide accompanied by formation of hemispherical structures due to volume expansion. Eventually, the aluminum completely transferred into alumina accompanied the end of the all anodic process.

4. Conclusions

We investigate an efficient strategy for obtaining the tantalum oxide nanodot arrays with anodic aluminum oxide as template. The nanodot is self-organized at bottom of the pores of alumina film by electrochemical anodization. The nanodot diameter demonstrated here ranges between 15 nm and 70 nm and density ranges between $10^{11}/cm^2$ and $10^{10}/cm^2$. In addition, the diameter and density of the nanodot can be controlled by various applied voltages. SEM and XPS were used to determine the microstructure and chemical composition of the nanodots. The nanodots are composed of nonstoichiometric TaO_x. Using this approach, it is expected that nanodot arrays of various oxide semiconductors can be achieved.

Acknowledgements

The authors thank the National Science Council, Taiwan, for financially supporting this research through contract NSC-94-2113-M-009-020.

References

[1] W. Lu, Z.Q. Ji, L. Pfeiffer, K.W. West, A.J. Rimberg, Nature 423 (2003) 422.
[2] T.C. Harman, P.J. Taylor, M.P. Walsh, B.E. LaForge, Science 297 (2002) 2229.
[3] D. Gammon, E.S. Snow, B.V. Shanabrook, Science 273 (1996) 87.
[4] S.Y. Chou, P.R. Krauss, P.J. Rrnstrom, Science 272 (1996) 85.
[5] R.G. Freeman, K.C. Grabar, K.J. Allison, R.M. Bright, J.A. Davis, A.P. Guthrie, M.B. Hommer, M.A. Jackson, P.C. Smith, D.G. Walter, M.J. Natan, Science 267 (1995) 1629.
[6] H. Roder, E. Hahn, H. Brune, J.P. Buchern, K. Korn, Nature 366 (1993) 141.
[7] R. Notzel, J. Temmyo, T. Tamamura, Nature 369 (1994) 131.
[8] H. Masuda, K. Fukuda, Science 268 (1995) 146.
[9] S.A. Sapp, B.B. Lakshmi, C.R. Martin, Adv. Mater. 11 (1999) 402.
[10] H.Q. Cao, Y. Xu, J.M. Hong, H.B. Liu, G. Yin, B.L. Li, C.Y. Tie, Z. Xu, Adv. Mater. 18 (2001) 1393.
[11] S.B. Lee, D.T. Mitchell, L. Trofin, T.K. Nevanen, H. Soderlund, C.R. Martin, Science 296 (2002) 2198.
[12] G. Che, B.B. Lakshmi, C.R. Martin, E.R. Fisher, R.S. Ruoff, Chem. Mater. 10 (1998) 26.
[13] H. Masuda, M. Satoh, Jpn. J. Appl. Phys. 35 (1996) L126.
[14] H. Masuda, K. Yasui, K. Nishio, Adv. Mater. 12 (2000) 1031.
[15] M.S. Sander, L.S. Tan, Adv. Funct. Mater. 13 (2003) 393.
[16] H. Masuda, F. Hasegwa, S. Ono, J. Electrochem. Soc. 144 (1997) L122.
[17] D. Course, Y.H. Lo, A.E. Miller, M. Course, Appl. Phys. Lett. 76 (2000) 109.
[18] A.I. Vorobyova, E.A. Outkina, Thin Solid Films 324 (1998) 1.
[19] D.J. Werder, R.R. Kola, Thin Solid Films 323 (1998) 6.
[20] V. Surganov, A. Mozalov, L. Lastochkina, J. Appl. Spectrosc. 65 (1998) 850.